Acta Orthop. Belg., 2022, **88**, 1-9

ORIGINAL STUDY

doi.org/ 10.52628/88.1.01

Anthropometric three-dimensional computed tomography reconstruction measurements of the acetabulum in children/adolescents

Ali Darwich, Mohamad Bdeir, Sonja Janssen, Stefan Schoenberg, Sascha Gravius, Ahmed Jawhar

From the Department of orthopaedic and trauma surgery, University Medical Centre Mannheim, Medical Faculty Mannheim, Heidelberg University, Germany

The key element for differentiation between normal anatomical variants and pathological deformities is the prior definition of normal ranges for anthropometric parameters of acetabulum according to each age group. Aim of the present study is to analyze the development of the acetabulum in children/adolescents by accurate anthropometric measurements using 3D-CT scans and determine the variations occurring depending on age, gender and/or side.

This retrospective observational study included 85 patients (170 hips) under 15 years of age (0-15) undergoing 1.5mm CT scanning for non-hip related reasons. The measurements were performed by 2 board-certified orthopaedic surgeons. Each year of life represented an age group forming a total of 16 groups. Median number of patients per age group was 12 (range 4-16). The anthropometric parameters included acetabular volume, inclination, version, depth (coronal and axial), width (coronal and axial), Tönnis angle as well as anterior and posterior acetabular sector angles. Mean values, range, standard deviation, p-values, intra- and interrater reliability were calculated.

All measurement values correlated significantly with age. Statistically, there was no side or gender related difference. Rapid growth phases were observed at the age of 11-12. The inter- and intrarater reliability was high (range ICC 0.8-0.99, Cronbach alpha 0.86-0.99, Bland-Altman good agreement).

The present data provides age- and gender-related normative values as well as growth phases describing

Declarations: Funding: The authors did not receive grants or outside funding of any kind in support of their research for the preparation of this manuscript.

Conflicts of interest/Competing interests: The authors declared no potential conflicts of interest with respect to the authorship and/or publication of this article.

Acknowledgements : The authors thank Dr. Svetlana Hetjens from the institute of medical statistics and biomathematics (Medical Faculty Mannheim of the University of Heidelberg, Germany) for her help in the statistical analysis.

Ethics approval: This study was performed in line with the principles of the Declaration of Helsinki. Approval was granted by the Ethics Committee of clinical research at our institution (Ethikkommission II, University Medical Centre Mannheim, Medical Faculty Mannheim, Heidelberg University, Theodor-Kutzer-Ufer 1-3, 68167, Mannheim, Approval 2016-870R-MA).

- Ali Darwich[1]
- Mohamad Bdeir[1]
- Sonja Janssen[2]
- Stefan Schoenberg[2]
- Sascha Gravius[1]
- Ahmed Jawhar[1,3]

[1]*Department of orthopaedic and trauma surgery, University Medical Centre Mannheim, Medical Faculty Mannheim, Heidelberg University, Germany.*

[2]*Clinic of Radiology and Nuclear Medicine, University Medical Centre Mannheim, Medical Faculty Mannheim, Heidelberg University, Germany.*

[3]*Department of Trauma, Orthopedics, Hand and Reconstructive Surgery, Klinikum Worms, Academic Teaching Hospital of the University Mainz, Worms, Germany.*

Correspondence : Ali Darwich, Institutional address: Theodor-Kutzer-Ufer 1–3, 68167 Mannheim, Germany, Phone: +49 621 383 2526, ORCID-ID: 0000-0001-9463-9638

E-mail: alidarwich@mail.com

acetabular morphology. It should help paediatricians as well as paediatric and orthopaedic surgeons as a tool for early diagnosis of deformity and guidance for possible procedures.

Keywords: Anthropometric; computed tomography; measurements; acetabulum; children.

INTRODUCTION

Depending on age and gender, the acetabular morphology, congruence and dimensions vary widely *(1)*. The key element for differentiation between normal or anatomical variants and abnormal or pathological deformities is the prior establishment and definition of normal ranges of anthropometric parameters according to each age group *(2)*. These ranges are crucial, especially in children, since a delayed recognition and treatment of these pathologies can have a dramatic negative effect on the clinical outcome. In children with DDH, which is considered as the predominant pre-arthrotic mechanism, a late diagnosis of the deformity allowing it to remain till adolescence or early adulthood, can lead amongst others to gait problems, reduced strength, limb length difference, higher rate of hip degeneration, functional non-structural scoliosis and back pain *(3)*. DDH is just one example of the many pathologies affecting the morphology of the acetabulum and causing disastrous complications in late childhood and early adulthood, hence the great importance of an early diagnosis of such conditions *(3)*.

Only few studies describe the complete morphology and anthropometry on 3D CT scans of the adult hip *(4, 5)*; comparable CT-based studies in childhood are lacking. The majority of previous publications used two-dimensional techniques to quantify deformities of the hip joint *(6, 7)*. However, these imaging methods showed limited precision when variations in patients´ anatomy or position during imaging were present, for example by pelvis rotation or inclination *(8)*. Therefore, many authors recommend the more precise computed tomography as a cross-sectional imaging technique, where the 3D-CT based anthropometry might be more suitable in defining anomalies and normal anatomic variations *(2)*.

Aim of the present study is to analyze the development of the acetabulum in children/adolescents at a broad age range by accurate anthropometric measurements using 3D-CT scans and to determine the variations that occur depending on age, gender and/or side.

MATERIALS AND METHODS

The morphology of the acetabulum including volumetric and linear dimensions was evaluated using an anonymized CT scan data base of children/adolescents < 15 years of age provided by the radiologists. The observational retrospective consecutive case series consisted of 170 hips (85 patients, 46 males and 39 females), with a median age of 6 ± 4.7 years (males 6 ± 4.5 years and females 8 ± 4.9 years) (range 0-15). Each year of life represented an age group: 0 referred to the first year of age, 1 referred to the 13th till the 24th month, 2 referred to the 25th till the 36th month etc., forming a total of 16 groups. Median number of patients per age group was 12 (range 4-16). In all cases included in the analysis, CT scanning was performed for reasons not related to the hip. All CT scans were clinically indicated, 33/85 (39 %) were done on patients with abdominal symptoms and 52/85 (61 %) were trauma-related scans. None of the patients included presented destructive arthritis of the hip, hip dysplasia, Perthes disease, slipped capital femoral epiphysis, osteonecrosis of the femoral head, tumours in the hip region, hip deformity, previous hip surgery or hip trauma.

All CT exams were first read by a board-certified radiologist (SJ) and a board-certified orthopaedic surgeon (AD) in consensus-reading to confirm the absence of hip trauma or deformity and for consecutive inclusion of the patient in this normative collective. Then the scans were read by two orthopaedic surgeons (AD and AJ) with 10 and 7 years of experience in hip pathologies and expertise in performing hip measurements blinded to each other's results. This study has been reported in line with the STROBE Statement *(9)*.

The scans were performed between 09/2008 and 09/2019 on different CT scanner systems (Siemens Emotion 16: 16-slice single-source CT, Siemens Somatom® Definition Flash: 2x128 slice dual-source CT, Siemens Somatom® Force: 2x192 slice dual-source CT) within our institution, in a standard supine position using a helical scanning technique with collimations of 0.6 mm or 1.2 mm and pitch factors from 0.55 to 3. All datasets enrolled in the analysis included the pelvis and both proximal femurs. Volume CT dose index (CTDIvol) range was 0.18 – 74.89 mGy, whilst one has to keep in mind that indications for CT were highly variable in the retrospective cohort analyzed. Slice thickness was 1.5mm or less with an increment equal or smaller than the slice thickness. The image data of the images was in DICOM (Digital Imaging and Communications in Medicine) format and processed on the aycan® workstation OsiriX (aycan Medical Systems®, Rochester, NY, USA), where all the reconstructions and measurements were carried out (Fig 1, 2).

A detailed list of the performed measurements is to be found in Table I.

All measurements were performed twice by the first author (AD) at a minimum interval of 3 months.

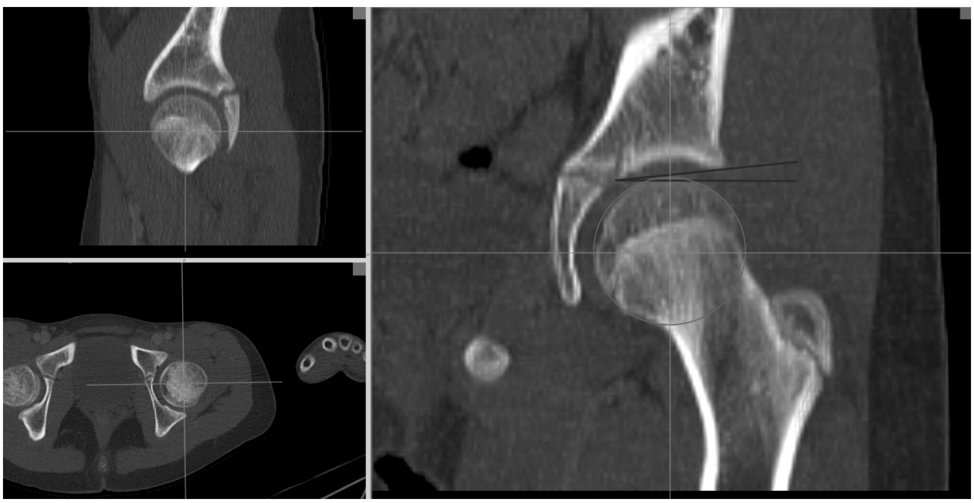

Figure 1. — Measurement method of Tönnis angle.

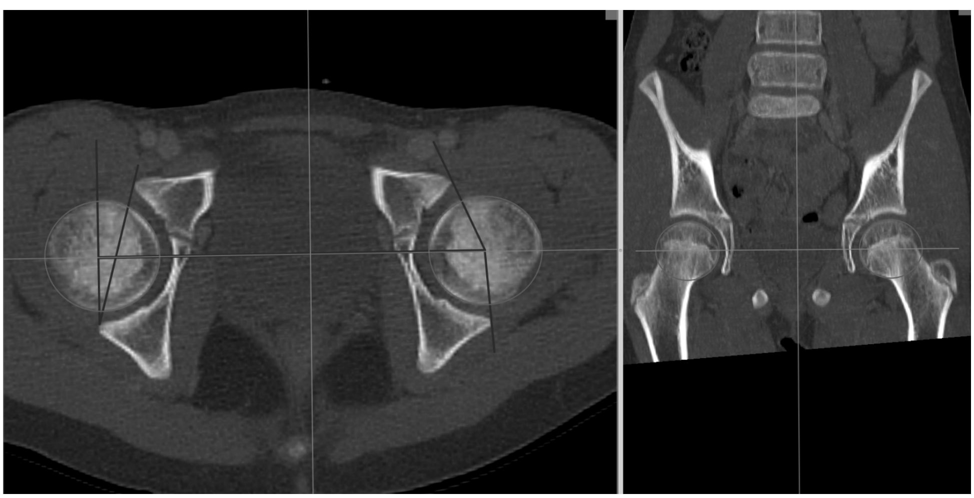

Figure 2. — Measurement method of anterior/posterior acetabular sector angle and acetabular anteversion ang.

Table I. — List of the performed measurements with description and plane configuration

Name of the measurement method	Unit	Figures describing the measurement method	Description of the measurement methods	Plane configuration
Volume acetabulum (VA)	cm^3	Supplement 2 Fig 1a	Boundaries of the acetabulum on the most cranial, most caudal and on every 2^{nd} axial slice were identified. A line connecting the anterior and posterior acetabular rims was used to close the entire acetabulum. Using the brush tool (aycan® workstation OsiriX), the area bounded by the acetabulum was manually filled on each slice (blue area). The areas of the missing slices were generated using the integrated ROI (Region of interest) function in aycan® workstation OsiriX. The acetabular volume (cubic millimetres) was calculated by adding all the areas [6, 42, 43].	Measurement: axial
Acetabular inclination (AI)	Degree	Supplement 2 Fig 2a	The angle between a parallel to the intercapital centre line and the line connecting the cranial and the caudal acetabular rims [6, 44].	Measurement: coronal Measurements are done on the coronal slice, in which the femoral head is most prominent Axial plane: The horizontal axis in the axial plane extends through both femur head centres. Sagittal plane: both axes go through the centre of the femur head
Tönnis angle (TA)	Degree	Supplement 2 Fig 3a	The angle between a parallel to the intercapital centre line and a line connecting to most lateral part of the cranial lip of acetabulum and the most medial part of the bony acetabular roof [6, 36, 45, 46].	
Anterior acetabular sector angle (AASA)	Degree	Supplement 2 Fig 5a	The angle between the intercapital centre line and a line extending from the corresponding femoral head centre and the anterior acetabular margin [6, 47].	Measurement: axial Coronal plane: The slice, in which the femoral heads are most prominent, is selected. The horizontal axis in the coronal plane extends through both femur head centres.
Posterior acetabular sector angle (PASA)	Degree	Supplement 2 Fig 5a	The angle between the intercapital centre line and a line extending from the corresponding femoral head centre and the posterior acetabular margin [6, 43, 48].	
Acetabular anteversion angle (AA)	Degree	Supplement 2 Fig 5a	The angle between the perpendicular to the intercapital centre line and a line connecting the anterior and the posterior acetabular rims [49].	
Acetabular depth ratio axial (ADRa)	-	-	The axial acetabular depth was defined as the length of a perpendicular extending from the line between the anterior and the posterior acetabular margin and the deepest most medial point of the acetabulum. The axial acetabular width was defined as the distance between the anterior and the posterior acetabular margins. The axial acetabular depth ratio was calculated by dividing the axial acetabular depth by the axial acetabular width multiplied by 1000 [43]	-

Table I. — List of the performed measurements with description and plane configuration -part 2

Acetabular depth ratio coronal (ADRc)	-	-	The coronal acetabular depth was defined as the length of a perpendicular extending from the line between the cranial and the caudal acetabular margin and the deepest most medial point of the acetabulum. The coronal acetabular width was defined as the distance between the cranial and the caudal acetabular margins. The coronal acetabular depth ratio was calculated by dividing the coronal acetabular depth by the coronal acetabular width multiplied by 1000 [43, 50]	-

The mean values of these 2 readings were used for further analysis including Intrarater reliability and presented as final values in this study. A second author (AJ) performed the same measurements independently and blinded to the results of the first observer. The plane configurations in each measurement were defined beforehand (Table I). Interrater reliability was performed comparing the measurements between the two observers (AD and AJ). Selection of the measurements was done according to their clinical relevance, mostly in the diagnosis and treatment of hip deformities such as hip dysplasia. The acetabular roof angle of Tönnis that evaluates the weight-bearing surface of the acetabulum and the acetabular depth ratio are some of the classical measurements used to diagnose hip dysplasia in the coronal plane *(10).* In the axial plane the anterior and posterior acetabular sector angles are usually used. These measurements are helpful not only in the diagnosis but also in the follow-up and the planning of complex three-dimensional osteotomies of the pelvis *(10)*.

Quantitative morphometric parameters were described using mean values and standard deviations (SD) and double-sided confidence intervals (CI) were calculated at 95 %. The statistical analysis was performed using Student´s t-test for parametric and Wilcoxon rank sum-test for nonparametric data. Correlations with other measurements were evaluated using the analysis of variance ANOVA taking into consideration gender, side, and age. Concerning the distribution of cases inside an age group, the number of available values per month was analyzed using a repeated ANOVA (procedure Proc Mixed). The reliability of the measurement methods was indicated as intraclass correlation coefficients (ICCs) as well as Cronbach`s alpha (Table II). Interclass variability was evaluated using Bland-Altman's approach *(11)*. Concerning growth phases, these were presented using sextic polynomial curves taking case dispersion in each age group into consideration. Because of the high number of performed correlations (Table III), the p value was adjusted according to Bonferroni´s method to correct increased error rates and the statistical significance was indicated by a p value of < 0.00021. Statistical analyses were performed using SAS software, release 9.4 (SAS Institute Inc., Cary, NC, USA) and SPSS software (Version 9, IBM, Chicago, IL, USA). Graphs were created using GraphPad Prism 8 (Version 8.4.2, San Diego, CA, USA).

This study was performed in line with the principles of the Declaration of Helsinki. Approval of this retrospective analysis was granted by the Ethics Committee of clinical research at our institution (Ethikkommission II, University Medical Centre Mannheim, Medical Faculty Mannheim, Heidelberg University, Theodor-Kutzer-Ufer 1-3, 68167, Mannheim, Approval 2016-870R-MA).

RESULTS

All measurements showed a statistically significant correlation with age (Table III). Acetabular

Table II. — Intrarater reliability

	Intraclass Correlation Coefficient	Cronbach`s alpha
VA	0.998107092	0.997726345
AI	0.877548601	0.92373519
TA	0.962070398	0.982154035
AASA	0.974162439	0.969997474
PASA	0.992986827	0.981764358
AA	0.985014053	0.980367019
ADRa	0.965966033	0.991842087
ADRc	0.934091555	0.975955926

Volume acetabulum VA, Acetabular inclination AI, Tönnis angle TA, Anterior acetabular sector angle ASAA, Posterior acetabular sector angle PASA, Acetabular anteversion angle AA, Acetabular depth ratio axial ADRa, Acetabular depth ratio coronal ADRc

Table III. — Correlation analysis

		Gender	Side	Age	VA	AI	TA	AASA	PASA	AA	ADRa	ADRc
VA	r			0.927	-	-0.509	-0.691	0.681	0.731	0.29	0.884	0.698
	p	0.6373	0.9467	< 0.001	-	< 0.001	< 0.001	< 0.001	< 0.001	< 0.001	< 0.001	< 0.001
AI	r			-0.462	-0.509	-	0.607	-0.244	-0.458	-0.197	-0.468	-0.444
	p	0.7302	0.3466	< 0.001	< 0.001	-	< 0.001	< 0.001	< 0.001	0.01	< 0.001	< 0.001
TA	r			-0.684	-0.691	0.607	-	-0.508	-0.630	-0.273	-0.736	-0.697
	p	0.3955	0.7679	< 0.001	< 0.001	< 0.001	-	< 0.001	< 0.001	< 0.001	< 0.001	< 0.001
AASA	r			0.644	0.681	-0.244	-0.508	-	0.614	-.0203	0.681	0.561
	p	0.3494	0.8841	< 0.001	< 0.001	0.001	< 0.001	-	< 0.001	< 0.001	< 0.001	< 0.001
PASA	r			0.751	0.731	-0.458	-0.63	0.614	-	0.533	0.824	0.680
	p	0.0002	0.8985	< 0.001	< 0.001	< 0.001	< 0.001	< 0.001	-	< 0.001	< 0.001	< 0.001
AA	r			0.352	0.290	-0.197	-0.273	-0.203	0.533	-	0.397	0.307
	p	0.0022	0.3864	< 0.001	< 0.001	< 0.001	< 0.001	< 0.001	< 0.001	-	< 0.001	< 0.001
ADRa	r			0.888	0.884	-0.468	-0.736	0.681	0.824	0.397	-	0.754
	p	0.0249	0.9484	< 0.001	< 0.001	< 0.001	< 0.001	< 0.001	< 0.001	< 0.001	-	< 0.001
ADRc	r			0.662	0.698	-0.444	-0.697	0.561	0.680	0.307	0.754	-
	p	0.1895	0.4815	< 0.001	< 0.001	< 0.001	< 0.001	< 0.001	< 0.001	< 0.001	< 0.001	-

Volume acetabulum VA, Acetabular inclination AI, Tönnis angle TA, Anterior acetabular sector angle ASAA, Posterior acetabular sector angle PASA, Acetabular anteversion angle AA, Acetabular depth ratio axial ADRa, Acetabular depth ratio coronal ADRc, Pearson coefficient r, statistical significance $p < 0.00021$

inclination and Tönnis angle (Fig 3) showed a decreasing trend with age. The remaining measurements increased with advancing age. None of the measurements showed gender or side dependent differences.

The number of available cases per month was analysed. The distribution between years was not significantly different ($p = 0.7891$). The intrarater reliability was high (range ICC 0.87-0.99, Cronbach alpha 0.92-0.99) (Table II). The interrater variability was evaluated using Bland-Altman's approach and showed good agreement with very few outliers.

A summary of the gender/age/side dependent differences of each measurement with and correlations with other measurements as well as their statistical significance is to be found in Table 3.

A detailed overview of all values of all measurements is to be found in Supplement 1.

A graphical presentation of the measurements is to be found in the graphs depicted in Supplement 2.

The performed Bland-Altman's plots are to be found in Supplement 3.

Concerning rapid growth phases, those were noted in almost all measurements at the age of 11-12. The corresponding polynomial curves are to be found in supplement 4.

DISCUSSION

A direct comparison of the present findings with results in the literature was not always possible. The few publications found in the literature *(6, 12-15)* analyzed only some of the measured parameters of the present work and included fewer and smaller age groups. For instance, Falliner et al. *(15)* measured parameters of children aged 6 weeks to 10 months, Sarban et al. *(6)* included only children aged 18 to 48 months, Jacquemier et al. *(12)* 12 to 39 months and Novais et al. *(14)* 10 to 17 years.

Some of the measured parameters such as acetabular volume and axial acetabular depth to width ratio were not contrasted with data from the literature, since no comparable studies measuring them in different age groups were found.

In the current study an overall mean acetabular inclination of 49.4 ± 4.5° was measured. The result is comparable with the values measured by Falliner et al. *(15)*, where an MRI-based mean inclination of 48.75° was observed but higher than the x-ray-based values presented by Tönnis et al. *(16)*, where an inclination angle after Ullmann and Sharp of 42 ± 1.3° was described. The measured mean Tönnis acetabular angle values were also slightly higher than the value presented by Tönnis et al. *(16)* (12.4 ± 4.6° versus 17.6 ± 2.5°). Novais et al. *(14)*) analyzed the CT scans of 27 asymptomatic patients aged 10 to 17 years; the mean Tönnis angle was lower with 6 ± 4°. The observed discrepancy may be due to the age difference between the patients included in each study (6 ± 4.7 years (range 0-15) versus 13 ± 2 years (range 10-17)). In this study a coronal acetabulum depth ratio of 288.8 ± 40.7 was measured, slightly lower than the one measured by Novais et al. *(14)*, where a coronal acetabulum depth ratio of 306 ± 28 was observed. The discrepancy here is also due to the mean age difference.

The mean acetabular anteversion angle of all patients in the present study was 13 ± 2.1°. The present data was in line with the CT-based mean value of 13.4 ± 2.8° reported by Sarban et al. *(6)*in children aged 18 to 48 months and the CT-based mean value of 13 ± 4° reported by Jacquemier et al. *(12)* in children aged 12 to 39 months.

Novais et al. *(14)* reported mean anterior acetabular sector angle and posterior acetabular sector angle values of 65 ± 7° and 90 ± 6°. The measurements are slightly higher than the ones measured in the present study (56.1 ± 5.2° and 79.4 ± 8.9° respectively).

Regarding growth pattern, the measured parameters showed rapid growth phases at the age of 11 and 12. These results correlate with those reported by Wegener et al. *(5)*, who investigated the development of joint space growth and observed rapid growth rates at the age of 12.

In the majority of previous publications, anthropometric measurements were performed using two-dimensional imaging techniques *(6, 7, 17)*. However, in this context the superiority of 3D CT is well established *(13, 18, 19)*. Therefore, amongst the many diagnostic modalities available and for more precise measurement, 3D CT, which is recommended by many authors *(20, 21)*, was chosen to be used in the present study.

The used CT scans were done for different reasons not related to the hip. This was not a limitation since all used scans included the acetabulum and had a slice thickness of 1.5mm or less.

A general limitation of CT-based methods is the potential underestimation of the cartilaginous structures. Regarding the inferiority of CT compared to MRI studies when assessing cartilaginous structures some authors propose MRI as a superior measurement method *(14, 22)*. However, patient`s position during MR-imaging affected the results. As most of the MRI sequences acquired in clinical routine today, have a very high in-plane resolution, yet are not isotropic or nearly isotropic, meaning that a-posteriori varying the cutting plane or angulations of a study is not possible which is a drawback compared to routine CT scans for this study design. In addition, in postoperative patients with remaining metallic particles the MRI examination was not performed due to expected artefacts and compromised evaluation. The development of metal artefact suppression sequences may be a promising way to address the latter issue *(23)*.

A great amount of data was gathered in the present study. However, one of the limitations is the rather small total number of cases in some age groups, which made the mapping of rapid growth phases very difficult. In the screening and inclusion of patients, ethnicity was not recorded. This may be also considered as a limitation, since the study was performed in a university hospital located in a metropolitan area with great ethnic variations.

Lastly, CT exams compared to conventional radiography generally have substantially higher radiation doses depending on the CT scanner generation, with the reproductive organs and bone marrow always being in the field-of-view for the indication of hip pathologies. As it is known that the stochastic risk for development of radiation-induced cancer or leukaemia is higher the younger the patient is, indication for CT scanning should be always made very carefully, sticking to the ALARA principle.

CONCLUSION

The present study provides new 3D CT-based data in the context of a comprehensive and quantitative anthropometric analysis of the acetabulum in children/adolescents of a broad age range between 0 and 15 years. This data can be considered as normative and should help paediatricians and orthopaedic/paediatric surgeons as a tool for early diagnosis of deformity and guidance for possible procedures as well as a mapping chart for rapid growth phases.

REFERENCES

1. Govsa F, Ozer MA, Ozgur Z. Morphologic features of the acetabulum. Arch Orthop Trauma Surg. 2005;125(7):453-61.
2. Chiron P, Espié A, Reina N, Cavaignac E, Molinier F, Laffosse JM. Surgery for femoroacetabular impingement using a minimally invasive anterolateral approach: analysis of 118 cases at 2.2-year follow-up. Orthop Traumatol Surg Res. 2012;98(1):30-8.
3. Thomas SR. A review of long-term outcomes for late presenting developmental hip dysplasia. Bone Joint J. 2015;97-b(6):729-33.
4. Ma H, Han Y, Yang Q, Gong Y, Hao S, Li Y, et al. Three-dimensional computed tomography reconstruction measurements of acetabulum in Chinese adults. Anat Rec (Hoboken). 2014;297(4):643-9.
5. Wegener V, Jorysz G, Arnoldi A, Utzschneider S, Wegener B, Jansson V, et al. Normal radiological unossified hip joint space and femoral head size development during growth in 675 children and adolescents. Clinical Anatomy. 2017;30(2):267-75.
6. Sarban S, Ozturk A, Tabur H, Isikan UE. Anteversion of the acetabulum and femoral neck in early walking age patients with developmental dysplasia of the hip. J Pediatr Orthop B. 2005;14(6):410-4.
7. Kim SS, Frick SL, Wenger DR. Anteversion of the acetabulum in developmental dysplasia of the hip: analysis with computed tomography. J Pediatr Orthop. 1999;19(4):438-42.
8. Zilber S, Lazennec JY, Gorin M, Saillant G. Variations of caudal, central, and cranial acetabular anteversion according to the tilt of the pelvis. Surg Radiol Anat. 2004;26(6):462-5.
9. von Elm E, Altman DG, Egger M, Pocock SJ, Gøtzsche PC, Vandenbroucke JP. The Strengthening the Reporting of Observational Studies in Epidemiology (STROBE) statement: guidelines for reporting observational studies. J Clin Epidemiol. 2008;61(4):344-9.
10. Mimura T, Mori K, Kitagawa M, Ueki M, Furuya Y, Kawasaki T, et al. Multiplanar evaluation of radiological findings associated with acetabular dysplasia and investigation of its prevalence in an Asian population: a CT-based study. BMC Musculoskeletal Disorders. 2017;18(1):50.
11. Bland JM, Altman DG. Measuring agreement in method comparison studies. Stat Methods Med Res. 1999;8(2):135-60.
12. Jacquemier M, Bollini G, Jouve JL, Volot F, Panuel M, Bouyala JM. [Acetabular anteversion in congenital luxation of the hip]. Rev Chir Orthop Reparatrice Appar Mot. 1995;80(1):22-7.
13. Li LY, Zhang LJ, Zhao Q, Wang EB. Measurement of acetabular anteversion in developmental dysplasia of the hip in children by two- and three-dimensional computed tomography. J Int Med Res. 2009;37(2):567-75.
14. Novais EN, Ferrer MG, Williams KA, Bixby SD. Acetabular Retroversion and Decreased Posterior Coverage Are Associated With Sports-related Posterior Hip Dislocation in Adolescents. Clin Orthop Relat Res. 2019;477(5):1101-8.
15. Falliner A, Muhle C, Brossmann J. Acetabular inclination and anteversion in infants using 3D MR imaging. Acta Radiol. 2002;43(2):221-4.

16. Tönnis D. Die angeborene Hüftdysplasie und Hüftluxation im Kindes- und Erwachsenenalter. 1 ed: Springer-Verlag Berlin Heidelberg; 1984.
17. Smith BG, Kasser JR, Hey LA, Jaramillo D, Millis MB. Postreduction computed tomography in developmental dislocation of the hip: part I: analysis of measurement reliability. J Pediatr Orthop. 1997;17(5):626-30.
18. Milone MT, Bedi A, Poultsides L, Magennis E, Byrd JW, Larson CM, et al. Novel CT-based three-dimensional software improves the characterization of cam morphology. Clin Orthop Relat Res. 2013;471(8):2484-91.
19. Murphy SB, Simon SR, Kijewski PK, Wilkinson RH, Griscom NT. Femoral anteversion. J Bone Joint Surg Am. 1987;69(8):1169-76.
20. Kim HT, Wenger DR. The morphology of residual acetabular deficiency in childhood hip dysplasia: three-dimensional computed tomographic analysis. J Pediatr Orthop. 1997;17(5):637-47.
21. Nakamura S, Yorikawa J, Otsuka K, Takeshita K, Harasawa A, Matsushita T. Evaluation of acetabular dysplasia using a top view of the hip on three-dimensional CT. J Orthop Sci. 2000;5(6):533-9.
22. Weishaupt D, Exner GU, Hilfiker PR, Hodler J. Dynamic MR imaging of the hip in Legg-Calvé-Perthes disease: comparison with arthrography. AJR Am J Roentgenol. 2000;174(6):1635-7.
23. Talbot BS, Weinberg EP. MR Imaging with Metal-suppression Sequences for Evaluation of Total Joint Arthroplasty. Radiographics. 2016;36(1):209-25.
24. Novais EN, Bixby SD, Rennick J, Carry PM, Kim YJ, Millis MB. Hip dysplasia is more severe in Charcot-Marie-Tooth disease than in developmental dysplasia of the hip. Clin Orthop Relat Res. 2014;472(2):665-73.
25. Fujii M, Nakamura T, Hara T, Nakashima Y, Iwamoto Y. Does radiographic coxa profunda indicate increased acetabular coverage or depth in hip dysplasia? Clinical orthopaedics and related research. 2015;473(6):2056-66.
26. Stelzeneder D, Hingsammer A, Bixby SD, Kim YJ. Can radiographic morphometric parameters for the hip be assessed on MRI? Clin Orthop Relat Res. 2013;471(3):989-99.
27. Ng KC, Lamontagne M, Adamczyk AP, Rakhra KS, Beaulé PE. Patient-specific anatomical and functional parameters provide new insights into the pathomechanism of cam FAI. Clin Orthop Relat Res. 2015;473(4):1289-96.
28. Tönnis D, Brunken D. Eine Abgrenzung normaler und pathologischer Hüftpfannendachwinkel zur Diagnose der Hüftdysplasie. Archiv für orthopädische und Unfall-Chirurgie, mit besonderer Berücksichtigung der Frakturenlehre und der orthopädisch-chirurgischen Technik. 1968; 64(3):197-228.